Lawrence Berkeley National Laboratory
LBL Publications

Title
Revisiting the t0.5 Dependence of SEI Growth

Permalink
https://escholarship.org/uc/item/0pq2f6r5

Journal
Journal of The Electrochemical Society, 167(9)

ISSN
0013-4651

Authors
Attia, Peter M
Chueh, William C
Harris, Stephen J

Publication Date
2020-01-07

DOI
10.1149/1945-7111/ab8ce4

Peer reviewed

Revisiting the $t^{0.5}$ Dependence of SEI Growth

View the article online for updates and enhancements.

CrossMark

Revisiting the $t^{0.5}$ Dependence of SEI Growth

Peter M. Attia,[1,*,z] **William C. Chueh,**[1,**] and **Stephen J. Harris**[1,2,z]

[1]*Department of Materials Science and Engineering, Stanford University, Stanford, California 94305, United States of America*
[2]*Materials Science Division, Lawrence Berkeley National Laboratory, Berkeley, California 94720, United States of America*

SEI growth in lithium-ion batteries is commonly assumed to scale with $t^{0.5}$, in line with simple models of diffusion-limited surface layer growth. As a result, this model is widely used for empirical predictions of capacity fade in lithium-ion batteries. However, the $t^{0.5}$ model is generally not theoretically sufficient to describe all of the various SEI growth modes. Furthermore, previous literature has not convincingly demonstrated that this model provides the best fit to measurements of SEI growth. In this work, we discuss the theoretical assumptions of the $t^{0.5}$ model, evaluate claims of $t^{0.5}$ dependence in six previously published datasets and one new dataset, and compare the performance of this model to that of other models. We find that few of the purported $t^{0.5}$ fits in literature are statistically justified, although $t^{0.5}$ generally describes SEI growth during storage better than SEI growth during cycling. Finally, we evaluate how the fitted exponents in the power-law models vary as a function of time, and we illustrate the limitations of using $t^{0.5}$ for prediction without validating its applicability to a particular dataset. This work illustrates the theoretical and empirical limitations of the $t^{0.5}$ model and highlights alternatives for more accurate estimates and predictions of SEI growth.
© 2020 The Author(s). Published on behalf of The Electrochemical Society by IOP Publishing Limited. This is an open access article distributed under the terms of the Creative Commons Attribution 4.0 License (CC BY, http://creativecommons.org/licenses/by/4.0/), which permits unrestricted reuse of the work in any medium, provided the original work is properly cited. [DOI: 10.1149/1945-7111/ab8ce4]

Supplementary material for this article is available online

Growth of the solid-electrolyte interphase (SEI), the product of electrolyte degradation products accumulating on the surface of the negative electrode, is among the most common lithium-ion battery degradation modes.[1–5] First reported by Peled[1] in 1979, SEI growth consumes active lithium and reduces the overall capacity of the battery. However, the SEI has historically been challenging to characterize.[2,5,6] A better understanding of the kinetics of SEI growth—including its dependence on time—will enable more accurate models and predictions of battery lifetime.

The time dependence of SEI growth has been extensively measured and modeled. Many experimental measurements of the time dependence of SEI growth on graphitic negative electrodes report a square-root dependence on time ($t^{0.5}$). These studies measure the capacity decrease[7,8] or impedance increase[9,10] during battery storage[7,9,10] and cycling,[8–10] attributing all degradation to SEI growth (in this work, "storage" refers to both open-circuit and constant-voltage conditions, often referred to as "calendar aging"). As a whole, $t^{0.5}$ models have been reported to perform well in capturing degradation kinetics during storage and gentle cycling, i.e. when degradation occurs primarily from SEI growth. Accordingly, many SEI growth models often assume $t^{0.5}$ scaling relationships,[7,11–15] which are often justified by comparison to simple diffusion-reaction models of surface layer growth.[16,17]

Given both the complexity of SEI growth and the variety of conditions under which it grows, it would be surprising if a model as simple as $t^{0.5}$ could accurately describe SEI growth in a wide range of circumstances. Furthermore, due to the historical precedent of the $t^{0.5}$ model, evaluating and comparing alternative models to experimental data is not common in the SEI literature. However, careful model selection is important both for validating scientific claims of the time dependence of SEI growth and for predicting capacity fade and resistance growth.

In this work, we revisit both the theoretical justification and experimental evidence for the $t^{0.5}$ dependence of SEI growth. We show that many of the assumptions in classic surface film growth models are not satisfied for SEI growth in typical battery systems. We then demonstrate how a comparison of multiple models can lead

to improved descriptions and predictions of SEI-induced capacity fade. We compare the performance of the $t^{0.5}$ model to two generalized power-law models for six literature datasets and one new dataset measuring the time dependence of SEI growth on carbon electrodes. Our results demonstrate that 0.5 often lies outside the 95% confidence intervals (CIs) of the fitted exponents in the generalized power laws, indicating that these $t^{0.5}$ models of SEI growth generally have poor statistical justification. Moreover, the generalized power laws often outperform the $t^{0.5}$ model in describing SEI growth. Finally, we evaluate the sensitivity of the power-law exponent to the timescale of the fit and illustrate the model selection process for empirical lifetime prediction. Overall, while the $t^{0.5}$ model performs adequately in some instances, we encourage the consideration of alternative models given the poor theoretical and empirical justification of the $t^{0.5}$ model in describing SEI growth.

Theoretical Justification for the $t^{0.5}$ Model

Comparison to classical surface film growth.—We start by revisiting the theoretical underpinnings of the $t^{0.5}$ model of SEI growth. Generally, a $t^{0.5}$ dependence is the signature of a diffusion-limited process, including random walks and the Sand and Cottrell equations in electrochemistry.[18] In the simplest case of diffusion-limited growth, the growth of surface films also scales with $t^{0.5}$. Evans[16] first presented a model of one-dimensional diffusion-reaction kinetics of surface film growth in 1924, which was adapted by later works such as Deal and Grove[17] to describe the thermal oxidation of silicon to form silicon oxide, $Si + O_2 \rightarrow SiO_2$ (Fig. 1). Neglecting the gas adsorption term, this model has three key assumptions:

A. The diffusion of oxidant (e.g. oxygen) is faster than the diffusion of substrate (e.g. silicon) through the surface film (e.g. SiO_2). As a result, the reaction occurs at the interface between the surface film and the substrate. The flux of oxidant through the film, J_{diff}, is given by Fick's first law, which can be approximated with a linear gradient at steady state:

$$J_{diff} = -D\left(\frac{\partial C}{\partial x}\right) \approx D\left(\frac{C_o - C_i}{x_{film}}\right) \qquad [1]$$

Here, D is the diffusivity of oxidant in the film; C_o and C_i are the concentrations of oxidant at the outer and inner interfaces, respectively; and x_{film} is the thickness of the surface film.

*Electrochemical Society Student Member.
**Electrochemical Society Member.
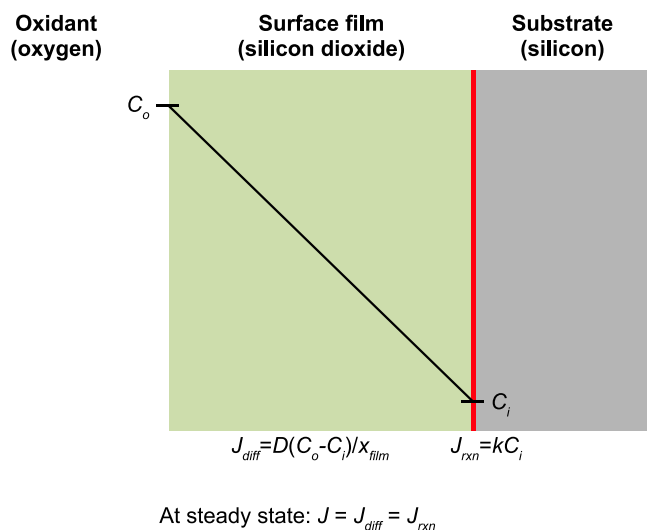zE-mail: peter.m.attia@gmail.com; sjharris@lbl.gov

Figure 1. Schematic of the Deal-Grove model of one-dimensional silicon oxidation, an example of a mixed reaction-diffusion process (scaling with $t^{0.5}$ at long times). Oxidation occurs when oxygen transports through the oxide and reacts with silicon to form silicon dioxide. Oxygen transport is diffusive and governed by Fick's first law (where the derivative is approximated as a difference at steady state), $J_{diff} = D\left(\frac{C_o - C_i}{x_{film}}\right)$, where D is the diffusivity of oxygen in silicon dioxide; C_o and C_i are the concentrations of oxygen at the outer and inner interfaces, respectively; and x_{oxide} is the thickness of the oxide layer. Oxygen reaction is approximated by a first-order kinetic model, $J_{rxn} = kC_o$, where k is the rate constant. At steady state, the diffusion and reaction fluxes are equal. The oxygen incorporation step at the gas-oxide interface is neglected in this depiction.

B. Oxidant that reaches the film/substrate interface chemically reacts with the substrate to form the surface film. The reaction flux, J_{rxn}, is a first-order reaction with respect to the oxidant:

$$J_{rxn} = kC_i \qquad [2]$$

Here, k is the rate constant. While film formation generally involves at least two reactants (e.g. Si and O), the rate is only governed by the concentration of one species if the concentration of the other species is in excess.

C. The system is at steady state (i.e. invariant with time), at which point the fluxes are equal:

$$J = J_{diff} = J_{rxn} \qquad [3]$$

If the surface film growth rate, dx_{oxide}/dt, is proportional to the steady-state flux J, we arrive at the following expression after integration with respect to time[17]:

$$x_{film}^2 + Ax_{film} = B(t + \tau) \qquad [4]$$

Here, A, B, and τ are constants. Thus, the thickness is predicted to scale with $t^{0.5}$ at large thicknesses and long times (i.e. $x_{film}^2 \propto t$ when $x_{film}^2 \gg Ax_{film}$ and $t \gg \tau$). This model successfully describes oxide layer growth on silicon under many conditons.[17]

Parabolic growth laws are commonly observed in oxidation processes, especially at high temperatures and large thicknesses (>600 nm).[19,20] However, a wide variety of other time dependences have been both theoretically derived and/or experimentally observed, including linear ($x_{film} \propto t$), cubic ($x_{film}^3 \propto t$), quartic ($x_{film}^4 \propto t$), logarithmic ($x_{film} \propto \ln t$), inverse logarithmic ($x_{film} \propto 1/\ln t$), and others.[19,20] Some factors that can lead to different growth modes include the nature of the transporting species, morphological features including cracks and grain boundaries, surface chemistry and orientation, space charge effects, and tunneling effects.[19,20] Furthermore, multiple growth modes will occur for the same system during different time regimes (i.e. initial, intermediate, and long-term growth). For example, the Deal-Grove model yields linear growth at short times (Eq. 4). Additionally, the Deal-Grove model breaks down for silicon in the initial stages of growth, where the growth rate exponentially decays with film thickness.[21]

For SEI growth, two main candidates are generally considered for the rate-limiting transporting species (at least in the one-dimensional case): electrons reacting at the electrolyte/SEI interface ("outer" SEI growth)[1,5,7,12] or solvent/salt anions reacting at the SEI/electrode interface ("inner" SEI growth).[12–14] This uncertainty in the true rate-limiting species leads to many possibilities for the rate-limiting transport step beyond pure diffusion. If the rate-limiting species is charged (e.g., electrons), more complex transport modes such as migration must be considered in addition to diffusion. Additionally, many of the factors that lead to non-parabolic time scaling in the oxidation literature may be relevant to SEI growth, such as space charge effects,[1] complex and three-dimensional morphologies,[5] electron tunneling,[12] complex (i.e. non-first-order) reaction orders,[3] and multiple growth regimes.[15] Thus, SEI growth is unlikely to be limited simply by diffusion, especially across different time and length scales.

SEI growth mechanisms.—Unlike surface film growth in passivation, SEI growth can be classified into three growth modes based on the sources and sinks of lithium ions and electrons: electrochemical, chemical, and thermal (Fig. 2). Each of these modes is expected to have a different dependence on time and other environmental parameters; however, only chemical SEI growth approximates classical film growth kinetics. A detailed description of reactions and interfaces present in electrochemistry is provided by Li and Chueh.[22]

Electrochemical SEI growth occurs when lithium ions from the electrolyte, electrons from the current collector, and electrolyte react to form SEI product. Electrochemical SEI growth requires a non-zero current, meaning it occurs during both cycling and constant-voltage conditions. In electrochemical SEI growth, the assumptions of the Deal-Grove model are often violated. Specifically, the transport gradients and reaction driving forces in a battery electrode (and its SEI) vary substantially over the course of a charge-discharge cycle, with timescales (~minutes–hours) typically much faster than those of SEI growth (~days–months). Thus, the substrate cannot be considered time invariant at typical cycling rates, and the steady-state assumption of classical surface-film growth models like Deal-Grove is broken. Furthermore, the SEI growth kinetics may be coupled to the intercalation process, as suggested by our previous work[26,27] showing that the SEI growth rate is much higher during lithiation than during delithiation. For these reasons, SEI growth during cycling bears little resemblance to Deal-Grove kinetics (i.e. its growth is not strictly diffusion-limited), and thus the $t^{0.5}$ scaling that results from these models is not applicable.

Chemical SEI growth occurs when neutral lithium (i.e. a lithium ion with an electron) in the electrode reacts with electrolyte. This mode of SEI growth occurs during both storage and cycling and is a dominant degradation mode during "calendar aging." This chemical deinsertion reaction does not involve net charge transfer, and its driving force is the chemical potential difference between lithium in the electrode and oxidized lithium in the SEI. In this way, chemical SEI growth is more analogous to chemical oxidation of metals and semiconductors. However, for graphite electrodes, the lithium concentration in the electrode decreases due to self-delithiation, which decreases the driving force and thus decreases the flux. Because the timescale of major changes to the system can be much faster than the timescale of SEI growth, the system cannot always be assumed to be in steady state. This violation may be neglected as long as the graphite electrode is in a phase transition, since the chemical potential of lithium in graphite during a phase transition is constant (and thus the SEI driving force is too). Keil et al.[28] confirmed that SEI growth rates in full cells largely track to the potential of the graphitic electrode; Single et al.[29] modeled found

a. Electrochemical SEI growth

b. Chemical SEI growth
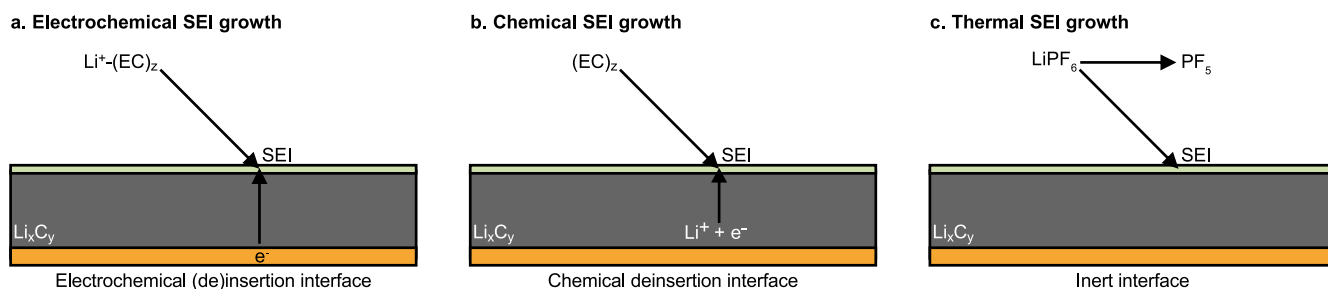

c. Thermal SEI growth

Figure 2. Schematics of three major SEI growth modes, which are governed by the sources and sinks of lithium ions and electrons. The specific SEI reaction/deposition interface is presented ambiguously due to our uncertainty in its actual location (i.e. "outer" or "inner" growth). (a) Electrochemical SEI growth. In this growth mode, lithium ions arrive at the interface from the electrolyte. Electrochemical SEI growth can occur whenever current is passed (cycling and constant-voltage conditions) and is a major contributor to capacity fade. Because an electrode cycling at typical rates experiences dramatic changes in its potential with time (at a timescale much faster than SEI growth), the steady-state assumption of classical surface-film growth models like Deal-Grove is broken, and thus the $t^{0.5}$ scaling that results from these models is not applicable. (b) Chemical SEI growth. In this growth mode, ambipolar lithium arrives at the interface from the lithiated electrode. Chemical SEI growth can occur during both cycling and storage and is a major contributor to capacity fade, particularly during "calendar aging." Chemical SEI growth bears some similarities to classical surface-film growth models like Deal-Grove. However, the self-delithiation of the electrode during this process can change the electrode composition and potential, which is dissimilar from classical surface-film growth models. (c) Thermal SEI growth. In this growth mode, SEI products arrive at the interface from the electrolyte. Thermal SEI growth occurs when electrolyte molecules spontaneously decompose and deposit SEI products on the electrode surface at high temperature; for example, lithium hexafluorophosphate salt (LiPF$_6$) decomposes at around 85 °C to produce LiF and PF$_5$.[23–25] This type of SEI growth can occur both during cycling and storage. Unlike chemical and electrochemical SEI growth, thermal SEI growth does not directly lead to capacity fade but can lead to impedance growth. Thermal SEI growth has little resemblance to classical surface-film growth models like Deal-Grove, and thus the $t^{0.5}$ scaling that results from these models is not applicable.

that the diffusion of lithium interstitials was the mechanism that best captured these data. Overall, chemical SEI growth bears some resemblance to Deal-Grove kinetics and thus has some theoretical basis for $t^{0.5}$ scaling.

Finally, thermal SEI growth occurs when electrolyte molecules spontaneously decompose and deposit SEI products on the electrode surface without exchanging lithium with the electrode. Thermal SEI growth can occur both during cycling and storage; the driving force for this reaction is the instability of electrolyte components at high temperature. For example, lithium hexafluorophosphate salt (LiPF$_6$) decomposes at around 85 °C, producing LiF and PF$_5$.[23–25] Unlike chemical and electrochemical SEI growth, thermal SEI growth does not directly lead to capacity fade but could lead to an increase in impedance. Thermal SEI growth is generally reaction-limited due to the initiating unimolecular reaction, although diffusion limitations could come into play (i.e. to carry product towards the surface within the electrolyte). Furthermore, the reaction occurs within the liquid electrolyte, not at an interface. Thus, thermal SEI growth has little resemblance to Deal-Grove kinetics, and thus the $t^{0.5}$ scaling that results from these models is not applicable.

Interaction between SEI and electrode chemistry.—One relevant system that satisfies the basic assumptions of the Deal-Grove model is SEI growth on lithium metal during rest. Specifically, the assumption of a constant reaction driving force assumption holds for lithium metal, but not graphite, because its electrode potential is constant with lithium composition. In his early SEI work, Peled's theoretical analysis[1] indicated that SEI growth on lithium metal should follow $t^{0.5}$ scaling at long times, but he reports that the observed power-law exponents for its growth actually range between 0.2–0.5. This result suggests that SEI growth mechanisms are likely more complex than standard diffusion.

Given the sub-0.5 observed exponents, we speculatively mention that the transport of electrons or solvent through the SEI may be a subdiffusive process. Subdiffusion is a case of "anomalous diffusion" in which the mean square displacement scales as $r^2 \sim t^{\beta}$, with $0 < \beta < 1$.[30] Subdiffusion is commonly reported in complex biological systems with "traps" and/or "dead ends" along the transport path[31]—a possibility for transport paths in the SEI.

Summary of the theoretical justification for $t^{0.5}$.—We suggest that our fundamental understanding of SEI growth kinetics is insufficient to support the theoretical description of a diffusion-limited
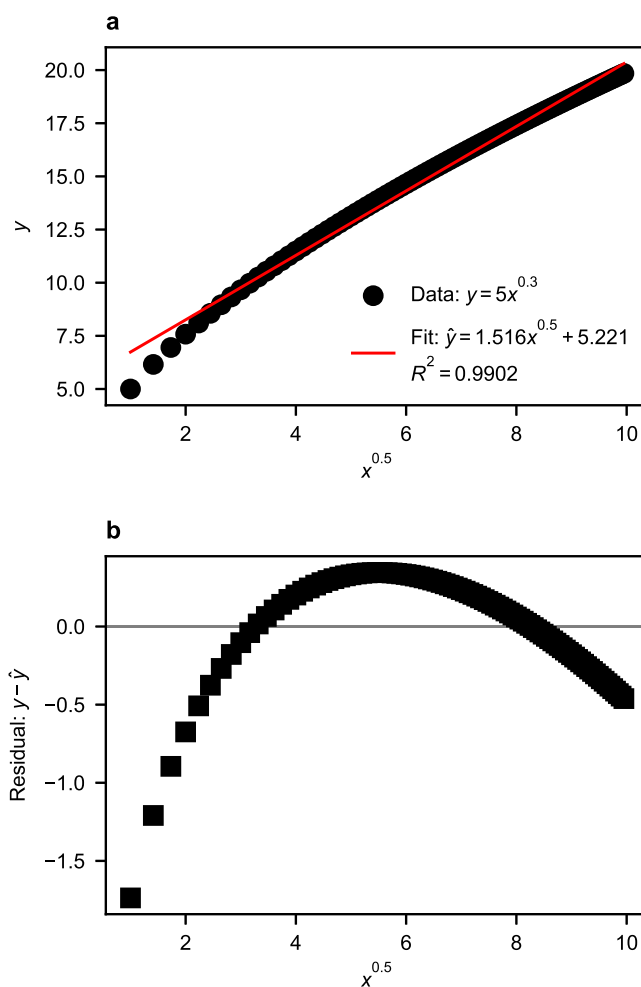

Figure 3. Problems with fitting power-law relationships with an assumed functional form such as $x^{0.5}$. (a) A dataset is generated by $y = 5x^{0.3}$ and fit to $\hat{y} = ax^{0.5} + b$. The model appears to fit the data well, with an R^2 value just above 0.99. (b) The residuals of the fit exhibit a systematic trend—a clear indication that the fit does not capture the true functional form of the data. This model will increasingly overestimate the true values of y as x increases.

process conforming strictly to $t^{0.5}$, even during later stages of growth. Furthermore, electrochemical and thermal SEI growth modes violate essential assumptions of the classical kinetics of surface layer growth. Thus, while $t^{0.5}$ may be sufficient for first-order estimates and predictions of SEI-driven capacity fade—particularly in the absence of experimental data—more advanced and complex SEI models that capture the complex behavior of the intercalating substrate during cycling[15,27] are important steps towards modeling SEI growth under relevant operating conditions. These efforts will be aided by advanced experimental characterization of SEI growth.

Empirical Evidence for the $t^{0.5}$ Model

In many contexts, the $t^{0.5}$ model has little theoretical justification to describe SEI growth. However, were this model to have broad empirical support, its use in practical applications would not be problematic and would perhaps be encouraged. However, as we show in this section, this model is often not the best choice for fitting experimental measurements of SEI growth. Maximizing accuracy is important for sensitive predictions of battery lifetime, both when incorporating models of SEI growth into physical degradation models and when extrapolating capacity fade data to predict future performance.

Statistical methodology.—A common practice in previous SEI work is to fit data to a $t^{0.5}$ model, such as $\hat{y} = at^{0.5}$ or $\hat{y} = at^{0.5} + b$, where $\hat{y}$ is some measure of capacity fade (variables with a "hat" represent fits, as opposed to measurements). These fits are then justified via a visual inspection of the trend line and a high coefficient of determination (R^2). However, this approach neither validates scientific claims of $t^{0.5}$ dependence, nor demonstrates a high-quality fit that captures the true functional form of the data. Claims of agreement between estimated and true parameters are incomplete without some measure of uncertainty of the estimated parameter. Additionally, R^2 has repeatedly been shown to be a misleading measure of goodness-of-fit, as notably illustrated by Anscombe's quartet.[32] Since R^2 specifically looks at the strength of the linear relationship between two variables, a fit can have a high R^2 yet fail to capture the underlying functional form of the data.

While many statistical tools for assessing goodness-of-fit are used today, one of the simplest yet most effective methods is graphical analysis of the residuals. Residuals are defined as the difference between the true and predicted values of the dependent variable. The main criterion to evaluate in residual analysis is randomness; any systematic trend in the residuals (autocorrelation) indicates that the fit has failed to capture the underlying structure of
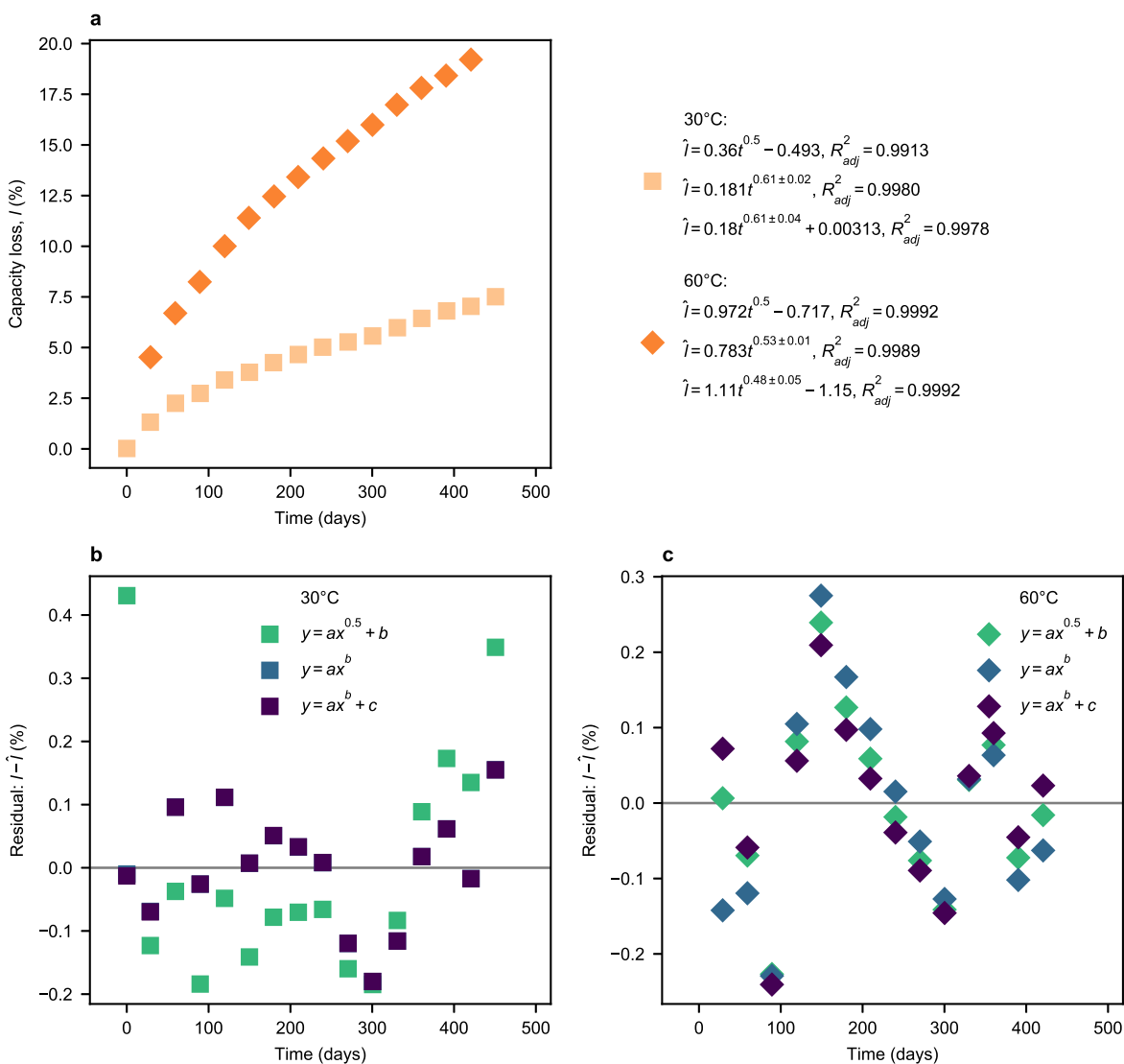

Figure 4. Comparison of $t^{0.5}$ and power-law fits to the data presented in Fig. 6 of Broussely et al.[7] (a) Capacity loss (*l*, %) vs time for two LiNi$_{0.81}$Co$_{0.09}$O$_2$/graphite [sic] cylindrical cells stored at a constant voltage of 3.8 V and temperatures of 30 °C and 60 °C ("Proto" cells). Both series are fit to three different models: $\hat{l} = at^{0.5} + b$, $\hat{l} = at^b$, and $\hat{l} = at^b + c$. Only one of the fitted exponents contains 0.5 in its 95% CI. The R^2_{adj} values of all models are comparable. (b), (c) Residuals of the three fits for (b) 30 °C and (c) 60 °C. The residuals of all models appear fairly random.
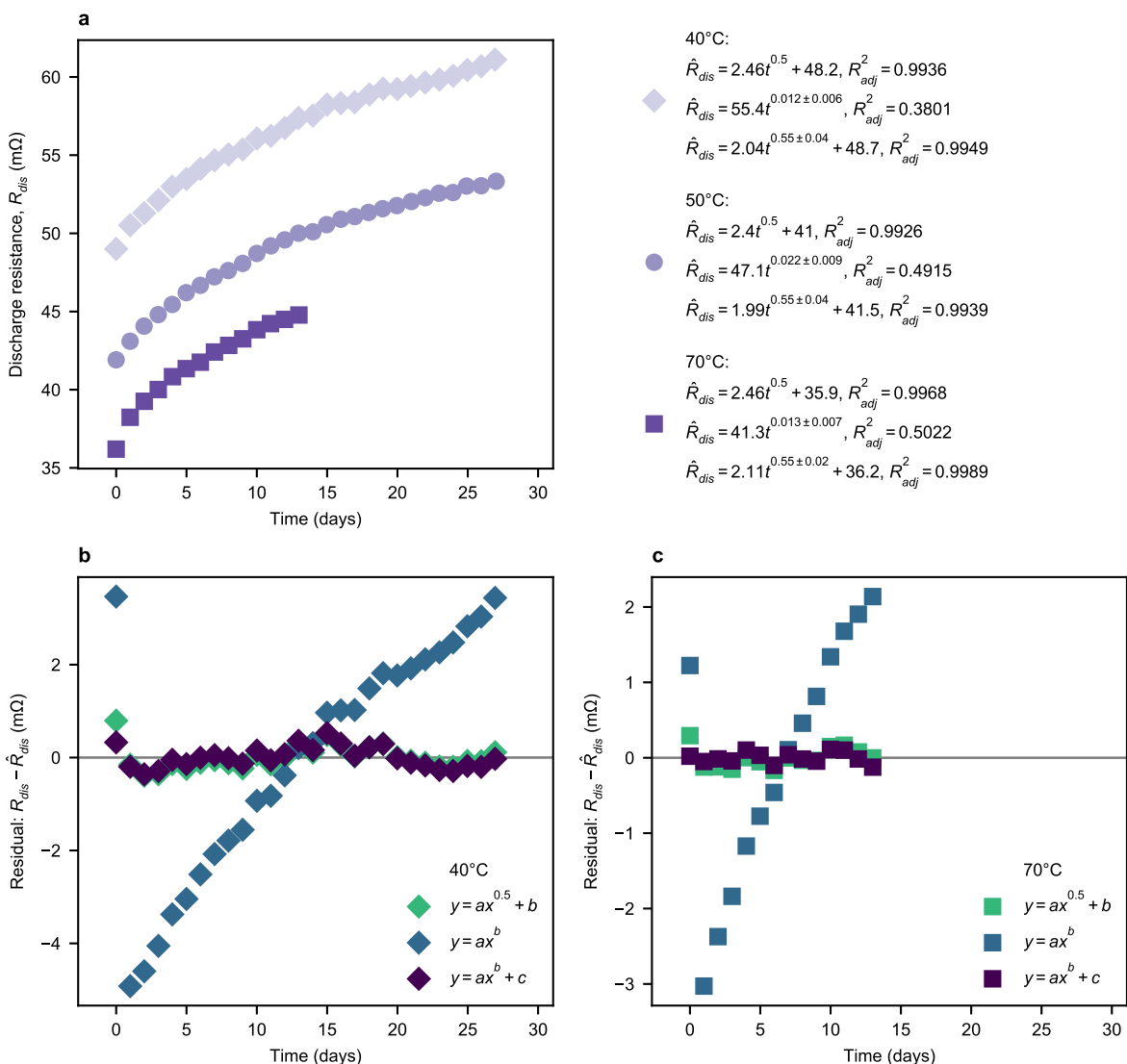
Figure 5. Comparison of $t^{0.5}$ and power-law fits to the data presented in Fig. 1 of Wright et al.[10] (a) Discharge resistance (R_{dis}, mΩ) vs time for three LiNi$_{0.8}$Co$_{0.1}$O$_2$/graphite cylindrical cells stored at temperatures of 40 °C, 50 °C, and 70 °C (the 60 °C data was difficult to extract). The three series are fit to three different models: $\hat{R}_{dis} = at^{0.5} + b$, $\hat{R}_{dis} = at^b$, and $\hat{R}_{dis} = at^b + c$. The exponents of the three-term power-law fit are close to 0.5, but 0.5 falls outside of the 95% CIs for all fitted exponents. The R^2_{adj} values of the $t^{0.5}$ and three-term power-law models are comparable. The two-term power-law fit performs poorly, likely due to the small variation in $\hat{R}_{dis}$ relative to its initial value. (b, c) Residuals of the three fits for (b) 40 °C and (c) 70 °C. The residuals of the $t^{0.5}$ and the three-term power-law models appear fairly random, while the two-term power-law model exhibits an obvious systematic trend.

the data. Residual analysis is useful as both a comparative and absolute tool for assessing goodness-of-fit. This method, while qualitative, offers an intuitive, visual understanding of model performance; in contrast, summary statistics like R^2 are quantitative metrics but can often be misleading.

Figure 3 illustrates both the pitfalls of relying on R^2 and "eyeballing" trend lines, and the advantages of residual analysis. We generated noiseless data with an $x^{0.3}$ functional dependence (Fig. 3a). A $x^{0.5}$ model, $y = ax^{0.5} + b$, appears to fit the data well: the trendline passes through the data, and the R^2 exceeds 0.99. However, graphical examination of the residuals reveals a systematic trend (Fig. 3b). Any curvature observed in the residuals (taking the shape of a "U" or "inverted U") indicates the presence of a nonlinear effect that is not captured by the model. Thus, this model does not capture the true functional form of the data; the model will be increasingly unreliable when used to predict the value of y at larger values of x.

In this section, we reevaluate the time dependence of SEI growth, and its purported $t^{0.5}$ dependence, for six selected datasets from the SEI literature and one new dataset. These datasets were selected for their prominence in the literature, likelihood of all measured

degradation being from SEI growth, and/or their data quality (i.e. large number of data points and low noise). However, we emphasize that other effects may convolute these measurements of SEI growth, such as SEI growth on the positive electrode in full cells, active material loss, impedance growth, current inhomogeneity,[33] electrode interactions ("cross-talk"),[34–37] and overhang effects.[38,39] We also selected datasets that quantify SEI growth by measuring either capacity fade or impedance growth, during either storage or cycling, and in either half cells and full cells. All datasets measure SEI growth via electrochemical techniques, which are generally precise (low noise). Electrochemical measurements capture the effects averaged over the entire cell, which ensures all regions of the cell are equally represented but may mask heterogeneities in local SEI growth rates.[33]

Our statistical approach has four components:

1. *Compare multiple models for each series.* Specifically, we choose three nonlinear univariate models for comparison: $\hat{y} = at^{0.5} + b$, $\hat{y} = at^b$, and $\hat{y} = at^b + c$. We emphasize that these models are empirical and have little theoretical
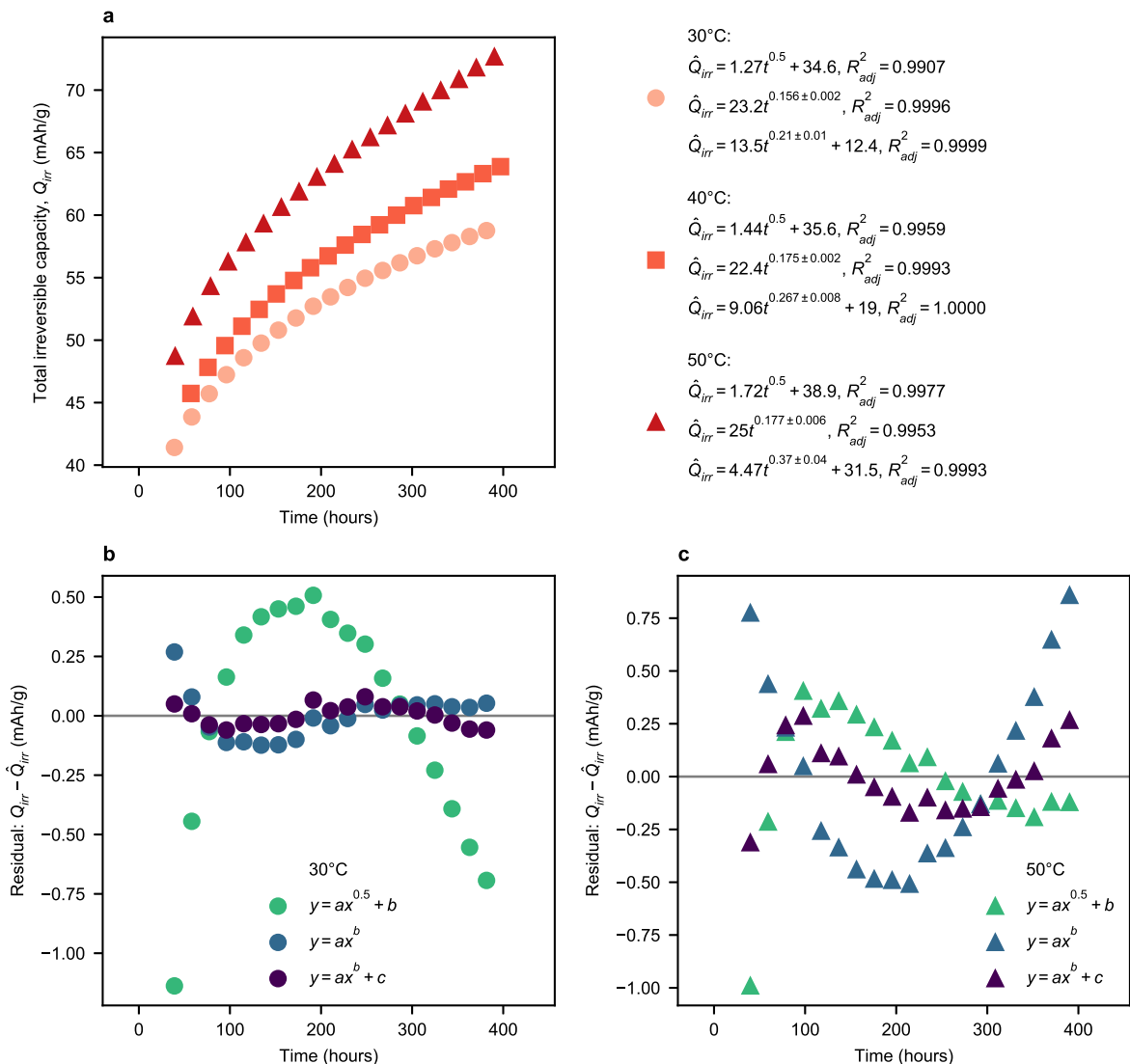
Figure 6. Comparison of $t^{0.5}$ and power-law fits to the data presented in Fig. 7 of Smith et al.[8] (a) Total irreversible capacity (mAh/g) vs time for graphite/lithium coin cells cycling at temperatures of 30 °C, 40 °C, and 50 °C and a rate of C/10 (the C/10 data was used since more data points were available). The data were measured using high-precision coulometry and temperature controlled to within ±0.1 °C. The three series are fit to three different models: $\hat{y} = at^{0.5} + b$, $\hat{y} = at^b$, and $\hat{y} = at^b + c$. The fits from the power-law models generally have higher R^2_{adj} values, and their exponents are much lower than 0.5. None of the fitted exponents contain 0.5 in their 95% CIs. Note that we evaluate additional functional forms for the 30 °C series in Fig. S1; again, none of the 95% CIs of the fitted exponents for the functional forms tested contain 0.5. (b), (c) Residuals of the three fits for (b) 30 °C and (c) 50 °C. The residuals of the $t^{0.5}$ model generally exhibit systematic trends, while the residuals of both power-law models exhibit stronger trends at 50 °C than at 30 °C.

justification; the generalized power-law fits were inspired by the many power-law scaling relationships in the oxidation literature,[19,20] and by no means is this model set exhaustive (we evaluate additional functional forms for one series in Fig. S1, which is available online at stacks.iop.org/JES/167/090535/mmedia). The use of power laws also provides a basis for evaluating claims of $t^{0.5}$ dependence. All models are fit with an unweighted nonlinear regression solver (as opposed to linear regression of transformed functions).

2. *Include 95% confidence intervals (CIs) for the exponents in the power-law models.* The 95% confidence interval of a parameter is the range of values for which the true value of parameter lies within, to 95% confidence. We include these to evaluate claims of $t^{0.5}$ dependence; if 0.5 falls outside the range of the 95% CI for the exponents in the power-law fits, the $t^{0.5}$ model is not statistically justified (at least with the selected power-law models). Here we use profile likelihood CIs calculated using the F test for nested models, which are asymmetric around the

estimated value of the parameter. These values are more representative of the true CIs for nonlinear regression models than the asymptotic approximate symmetrical CIs, which always underestimate the true CI.[40–42] However, we found that the difference between the two methods was negligible for these datasets; as a result, we represent the 95% CIs symmetrically (i.e. using ±) for simplicity.

3. *Include adjusted R^2 (R^2_{adj}) for each fit.* Specifically, we calculate R^2_{adj} between the predicted response and the observed response, as opposed to between the observed response and the predictor (which is not valid for nonlinear regression). One problem with R^2 as a comparative metric is that it always increases with more parameters, which unfairly penalizes simpler models. In contrast, R^2_{adj} penalizes the use of additional fitting terms. We include this metric for three purposes: first, to compare models via an (overly) simple summary statistic; second, to illustrate that high values of R^2_{adj} can obtained for most fits, making it an unreliable metric of goodness-of-fit; and third, to illustrate how
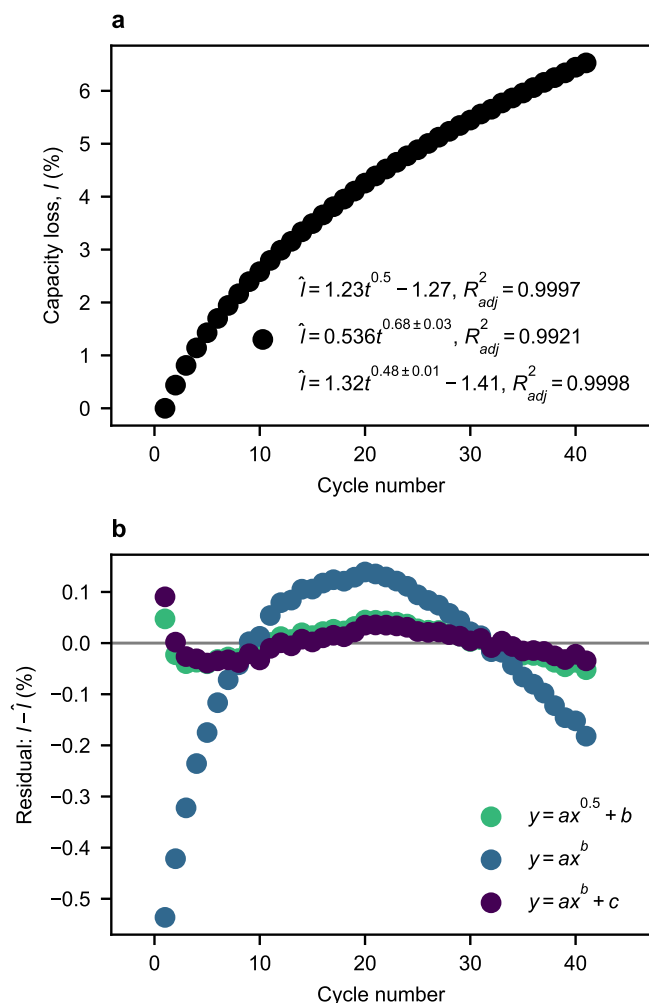
a

$$\hat{l} = 1.23t^{0.5} - 1.27, R_{adj}^2 = 0.9997$$

$$\hat{l} = 0.536t^{0.68 \pm 0.03}, R_{adj}^2 = 0.9921$$

$$\hat{l} = 1.32t^{0.48 \pm 0.01} - 1.41, R_{adj}^2 = 0.9998$$

b

$y = ax^{0.5} + b$
$y = ax^b$
$y = ax^b + c$

Figure 7. Comparison of $t^{0.5}$ and power-law fits to the data presented in Fig. 8 of Smith et al.[47] (a) Capacity loss (l, %) vs cycle number for a LiMn$_2$O$_4$/graphite cylindrical cell cycling at C/14 and 40 °C. The data were measured using high-precision coulometry. The data are fit to three different models: $\hat{l} = at^{0.5} + b$, $\hat{l} = at^b$, and $\hat{l} = at^b + c$. The fits from the $t^{0.5}$ and three-term power-law models have high and comparable R_{adj}^2 values. None of the fitted exponents contain 0.5 in their 95% CIs. (b) Residuals of the three fits. The residuals of all fits exhibit systematic trends, but the trends in the two-term power-law model are most pronounced.

the models with the best correlative metrics (such as R_{adj}^2) may not have the bets *predictive* metrics (relevant if prediction is an objective of the fitting process).

4. *Include residual analysis for selected series from all datasets.* Note that residual analysis will always favor higher-parameter models, since this method has no penalty for overfitting. Unlike our use of R_{adj}^2 as a comparative metric, we use residual analysis as an absolute method for determining goodness-of-fit. That is, we should use a model with enough complexity to obtain an acceptable fit, but not overly simple to avoid underfitting nor overly complex to avoid overfitting.

All literature data were extracted from the published figures using WebPlotDigitizer,[43] which has been shown to be a reliable data extraction method.[44,45] We found that triplicate extractions agreed within <0.1% on average (relative standard error). All data and code used in this analysis are publicly available online.[46]

Literature review.—We now reevaluate the time dependence of SEI growth in each of the seven datasets. We mention that these results may be sensitive to data manipulations such as baseline

subtraction and normalization; for instance, a baseline subtraction will change the goodness-of-fit for the two-term power-law model, but not for the selected $t^{0.5}$ model and the three-term power-law model (since both have intercept terms).

Broussely et al.[7] performed some of the earliest published studies of capacity fade in lithium-ion batteries. Figure 6 of Broussely et al.[7] presents two LiNi$_{0.81}$Co$_{0.09}$O$_2$/graphite [sic] cylindrical cells stored at a constant voltage of 3.8 V and temperatures of 30 °C and 60 °C ("Proto" cells), with periodically evaluated capacities. The timescale of this dataset exceeds 400 d.

We evaluated fits to these data in Fig. 4. We find that the R_{adj}^2 values of all models are comparable, and the residuals of all fits to both datasets generally appear random. The exponents of the power-law fits are quite close to 0.5 (maximum deviation = 0.11). However, only one fitted exponent (three-term power law, 60 °C) contains 0.5 in its 95% CIs. In this case, the $t^{0.5}$ model actually yields similar results to the generalized power-law models; however, strictly speaking, an exponent of 0.5 is only justified in one of the four fits.

Wright et al.[10] also performed early studies of SEI growth in LiNi$_{0.8}$Co$_{0.2}$O$_2$/graphite cylindrical cells during storage and cycling. This work quantified SEI growth using the increase in the discharge resistance (R_{dis}) from a reference performance test. The timescale of these experiments is approximately one month.

We evaluated the storage data at temperatures of 40 °C, 50 °C, and 70 °C from Fig. 1 of Wright et al.[10] in Fig. 5. The R_{adj}^2 values of the $t^{0.5}$ and three-term power-law models are comparable, and the residuals of the $t^{0.5}$ and three-term power-law models are comparable and generally random. The exponents of the three-term power-law fit are close to 0.5 (maximum deviation of 0.05). Again, however, none of the 95% CIs of the fitted exponents contain 0.5. The two-term power-law fit performs poorly, which is likely due to the non-zero initial value of the data; in other words, a constant offset is needed to accurately fit this dataset. Again, we find that while the $t^{0.5}$ model performs similarly to the three-term power-law model, an exponent of 0.5 is technically not statistically justified for all three series.

Smith et al.[8] published seminal work on capacity fade in graphite/lithium coin cells during low-rate cycling (C/24–C/10). In this dataset, the capacity loss was carefully measured using high-precision coulometry. Additionally, by using a lithium metal counter electrode, the electrochemically-measured capacity loss can be attributed solely to the graphitic electrode. Because the total capacity of the lithium metal counter electrode is much larger than that of the carbon electrode, its potential remains essentially constant during low-rate cycling (even accounting for the redox potentials of SEI reactions). Additionally, chemical SEI growth of lithium metal does not influence the measured electrochemical signals. Thus, the only measurable source of lithium inventory loss is SEI growth of the graphite electrode. The cells were temperature controlled at various temperatures to within ±0.1 °C, and the timescale of these experiments is approximately 17 d.

We evaluated the C/10 cycling data at temperatures of 30 °C, 40 °C, and 50 °C from Fig. 7 of Smith et al.[8] in Fig. 6. The fits from the power-law models generally have higher R_{adj}^2 values, and their exponents are much lower than 0.5 (ranging from 0.16 to 0.37). None of the 95% CIs of the fitted exponents contain 0.5. Furthermore, we evaluate additional functional forms for the 30 °C series in Fig. S1; none of the 95% CIs of the fitted exponents for the functional forms tested contain 0.5. The residuals appear highly non-random for the $t^{0.5}$ model of the 30 °C series; for the 50 °C series, all the residuals appear non-random. Overall, the $t^{0.5}$ model performs poorly relative to generalized power-law models, particularly for the 30 °C and 40 °C series.

Smith et al.[47] also performed capacity fade studies in commercial cells during cycling using high-precision coulometry. Figure 8 of this work presents capacity fade measurements in a LiMn$_2$O$_4$/graphite 18650 cylindrical cell cycled at C/14 and 40 °C. The timescale of this experiment is approximately 48 days.
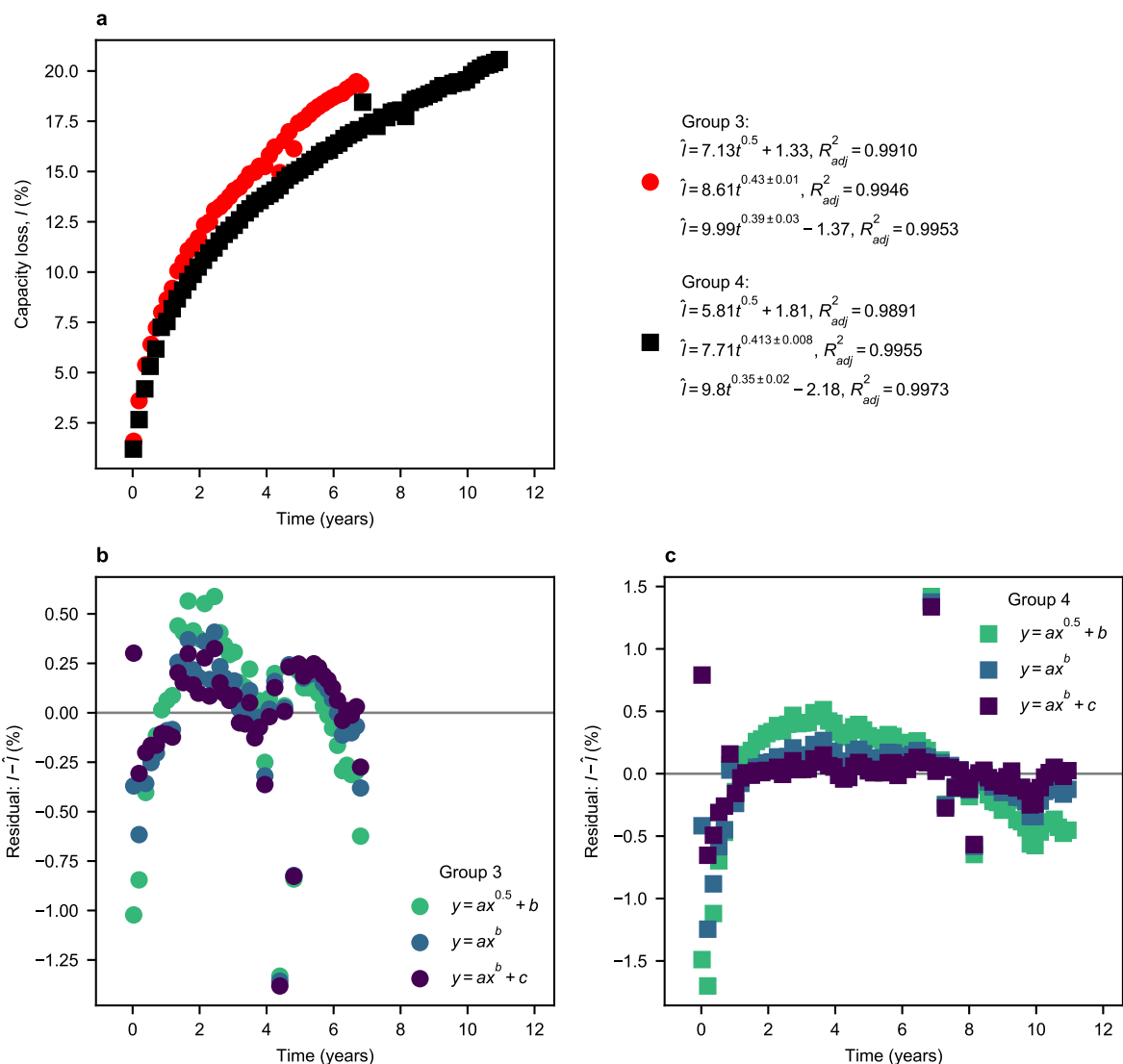
Figure 8. Comparison of $t^{0.5}$ and power-law fits to the data presented in Fig. 2a of Fathi et al.[48] (a) Capacity loss (l, %) vs time for LiCoO$_2$/graphite prismatic cells cycling at rates of ~C/6 and ~C/150 for charge and discharge, respectively, and a temperature of 37 °C. One cell from each aging groups (G$_3$ and G$_4$) was selected for analysis. The two series are fit to three different models: $\hat{l} = at^{0.5} + b$, $\hat{l} = at^b$, and $\hat{l} = at^b + c$. The fits from the power-law models have somewhat higher R^2_{adj} values, with exponents of ~0.4. None of the fitted exponents contain 0.5 in their 95% CIs. The exponents from cells from the same group do not vary substantially, indicating cell-to-cell variation is not a major effect in exponent determination. Note that the y-axis was flipped from the original figure. (b), (c) Residuals of the three fits for (b) Group 3 and (c) Group 4. The residuals of all fits are fairly random, with the exception of the $t^{0.5}$ model fit for Group 4.

We evaluated the data from Figure 8 of Smith et al.[47] in Fig. 7. The $t^{0.5}$ and the three-term power-law models have comparable R^2_{adj} values and residuals. The fitted exponent from the three-term power-law model is 0.48 ± 0.01. In contrast, the two-term power-law model has a considerably lower R^2_{adj} value and more non-random residuals. Overall, the $t^{0.5}$ model performs comparably to the generalized power-law models, although 0.5 is just outside of the 95% CI of the exponent in the three-term power-law model. However, we note that the residuals for all models have a systematic trend ("inverted U" shape), implying that a different model yet may best capture the true functional form of the data.

Fathi et al.[48] also used high-precision coulometry to study capacity loss during cycling. This dataset is notable due to its experimental timescale of over ten years. Figure 2 of Fathi et al.[48] displays capacity fade data from LiCoO$_2$/graphite prismatic cells cycling at rates of ~C/6 and ~C/150 for charge and discharge, respectively, and a temperature of 37 °C.

We evaluated one cell each from the two aging groups (G$_3$ and G$_4$) in Fig. 8. Here, we plot $1 - Q/Q_0$, instead of Q/Q_0, so that the data is monotonically increasing and consistent with the other

datasets. The fits from the power-law models have somewhat higher R^2_{adj} values, with fitted exponents of ~0.4. However, none of the 95% CIs of the fitted exponents contain 0.5. The cell from Group 3 exhibits random residuals for all series; in contrast, the cell from Group 4 exhibits systematic trends in the residuals, particularly for the $t^{0.5}$ model. Overall, generalized power-law models offer at least slightly better performance than the $t^{0.5}$ model.

Next, we evaluate a dataset from our own work[26] on capacity fade of carbon black/lithium coin cells during cycling. Carbon black has high surface area and thus grows large amounts of SEI. These cells were cycled at C/20 and a temperature of 30 °C; additional experimental conditions are detailed in Attia et al.[26] Similar to Smith et al.,[8] the SEI growth on lithium in carbon/lithium half cells is not measured, so all measured lithium inventory loss can be attributed to the carbon electrode. To study the effect of cell-to-cell variation in fitting exponents, we selected three cells with identical cycling conditions. Note that the high initial value arises from the anomalous first-cycle SEI growth reaction.[26,49]

The fits to this dataset are presented in Fig. 9. The power-law fits have much higher R^2_{adj} values and more random residuals than the
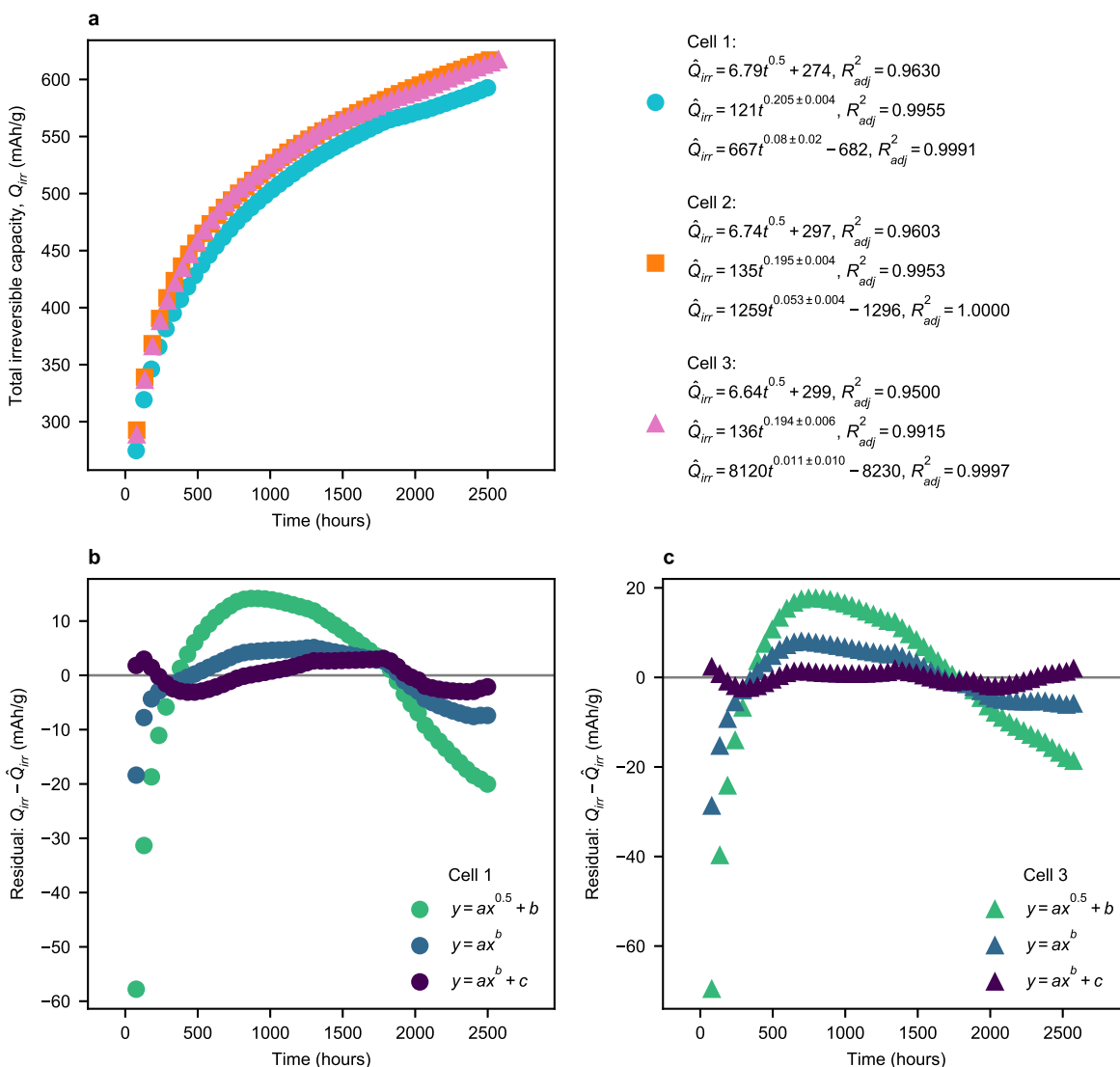
Figure 9. Comparison of $t^{0.5}$ and power-law fits to capacity fade in carbon black during cycling. (a) Total irreversible capacity (Q_{irr}, mAh/g) vs time of three carbon black/lithium coin cells cycling at C/20 and a temperature of 30 °C. Additional experimental conditions are detailed in Attia et al.[26] The three series are fit to three different models: $\hat{y} = at^{0.5} + b$, $\hat{y} = at^b$, and $\hat{y} = at^b + c$. The fits from the power-law models have much higher R^2_{adj} values, with exponents of ∼0.2 for the two-term power-law model. All fitted exponent values are far from 0.5; none of the fitted exponents contain 0.5 in their 95% CIs. The large and offsetting a and c terms of the three-term power-law model indicate that this fit is somewhat unreliable. The exponents from these nominally identical cells do not vary substantially, indicating cell-to-cell variation is not a major effect in exponent determination. (b), (c) Residuals of the three fits for (b) Cell 1 and (c) Cell 3. The residuals of the $t^{0.5}$ model exhibit the most pronounced systematic trends in both cells.

fits from the $t^{0.5}$ model. The exponents are approximately 0.20 for the two-term power-law models, and 0.5 is well outside of the 95% CIs of all fitted exponents. The large and offsetting a and c terms of the three-term power-law model indicate that these parameters may be difficult to physically interpret. The exponents from these nominally identical cells do not vary substantially, indicating cell-to-cell variation is not a major effect in exponent determination for these cells. Overall, the $t^{0.5}$ model performs poorly for this dataset.

Finally, we evaluate a previously unpublished dataset from our own work on capacity fade of carbon black/lithium coin cells during open-circuit storage. As the carbon black electrode delithiates during rest to grow SEI via a chemical reaction, the electrode potential decreases. Thus, we can combine the voltage vs time during the rest with the voltage vs capacity during delithiation to obtain SEI capacity vs time during rest. A similar technique was previously proposed by Levi et al.[50] In our experiments, we cycle each cell for a predetermined number of cycles between 0.01 V and 2.0 V at C/10 and 30 °C, ending in the fully lithiated state; subsequently, we measure voltage vs time and convert to SEI capacity vs time. This experiment allows us to evaluate both the time dependence of SEI growth in carbon black during storage, as well as how this time dependence changes as a function of "pre-cycling" (i.e. previous SEI growth). The raw voltage vs time and voltage vs capacity traces are presented in Fig. S2; details about cell construction and experimental apparatus are identical to Attia et al.[26]

The fits to this dataset are presented in Fig. 10. Generally, the power-law fits have higher R^2_{adj} values and more random residuals than fits from the $t^{0.5}$ model. All estimated exponent values are less than 0.5, and 0.5 is well outside of the 95% CIs of all fitted exponents. Interestingly, the exponents approach 0.5 for cells with more pre-cycling. This result could indicate that SEI growth approaches the diffusion-limited regime as the SEI gets thicker. However, the lower values of the exponent (∼0.3) for cells with little pre-cycling are surprising; exponent values above 0.5 are typically expected in the reaction-limited regime. Overall, the $t^{0.5}$ model performs poorly for this dataset. Importantly, this experiment highlights how chemical SEI growth on carbon electrodes diverges from the theory of classical diffusion-limited growth kinetics: the
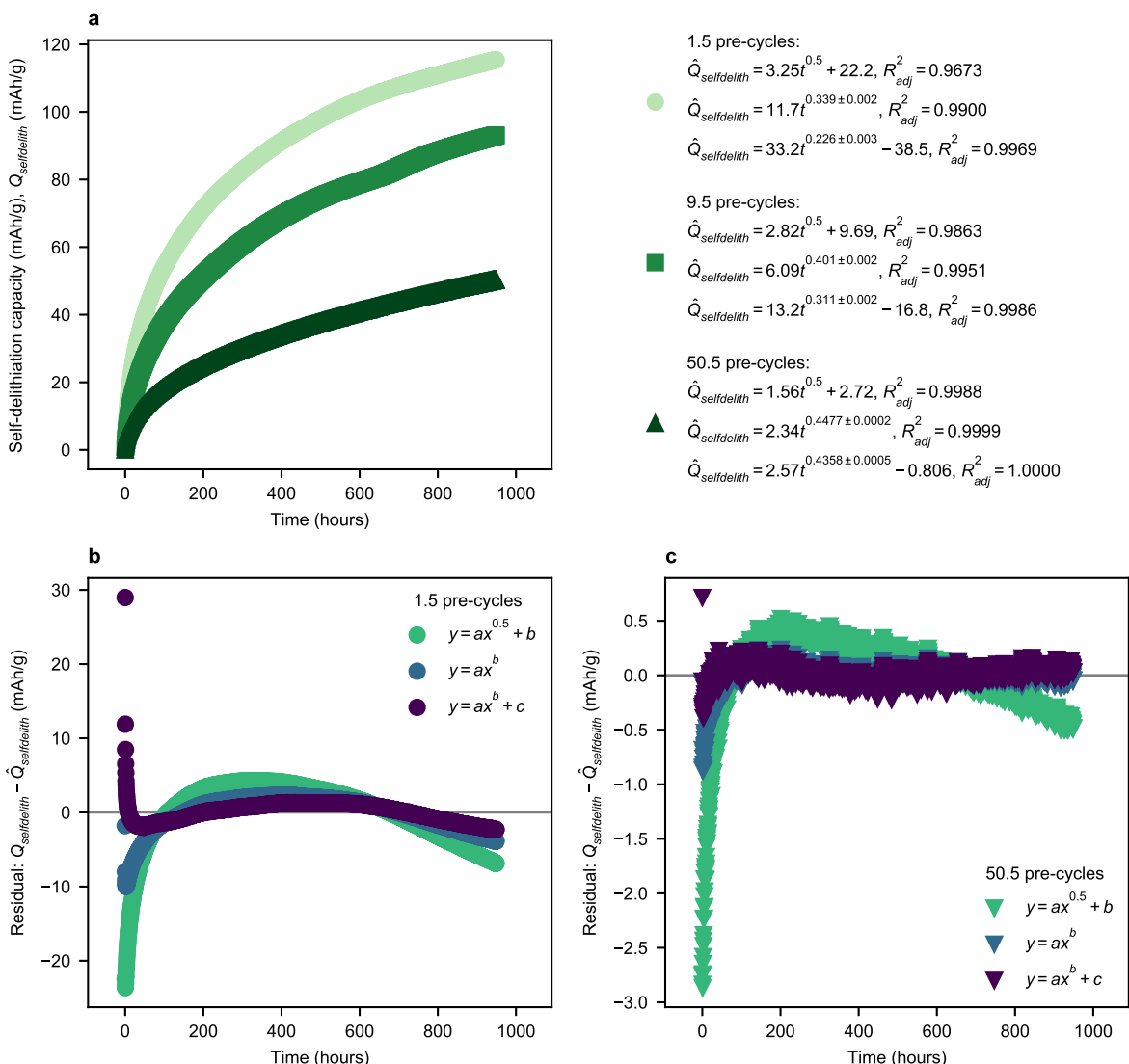
Figure 10. Comparison of $t^{0.5}$ and power-law fits to capacity fade in carbon black during open-circuit storage. (a) Self-delithiation capacity ($Q_{self\text{-}delith}$, mAh/g) vs time of three carbon black/lithium coin cells resting at a temperature of 30 °C. "Pre-cycles" refers to the number of cycles performed before the rest; the fractional cycle indicates that the pre-cycling ended with the electrode in the lithiated state. The pre-cycling occurred between 0.01 V and 2.0 V at C/10 and a temperature of 30 °C. The raw data used to derive these traces are presented in Fig. S2; additional experimental conditions are detailed in Attia et al.[26] The three series are fit to three different models: $\hat{y} = at^{0.5} + b$, $\hat{y} = at^{b}$, and $\hat{y} = at^{b} + c$. The fits from the power-law models have higher R^2_{adj} values than the $t^{0.5}$ model. All fitted exponent values are far from 0.5; none of the fitted exponents contain 0.5 in their 95% CIs. Interestingly, the exponents approach 0.5 with increasing pre-cycling. (b), (c) Residuals of the three fits for the cells with (b) 1.5 pre-cycles and (c) 50.5 pre-cycles. The residuals of the $t^{0.5}$ model exhibit the most pronounced systematic trends in both cells. The residuals are lower in magnitude for the cell with 50.5 pre-cycles than the cell with 1.5 pre-cycles.

electrode potential, and thus the driving force, changes as the SEI grows due to self-delithiation. This effect is especially pronounced in carbon black electrodes, which does not have phase transitions and thus always has fairly large changes in voltage per unit of capacity (see Fig. S1b).

Summary of literature re-analysis.—The experimental conditions from the literature datasets, and our results from the fits, are summarized in Table I. Overall, only 1 of the 17 series considered in this work (and 1 of the 28 power-law fits) had a fitted exponent with 0.5 contained in its 95% CI. Additionally, in Fig. S1, we confirm that other variations of exponential functional forms also do not contain 0.5, at least for the C/10, 30 °C series in Smith et al.[8] Our results suggest that the statistical justification for the $t^{0.5}$ model in describing SEI growth is weak. Additionally, few factors emerge as strongly correlated with high performance of $t^{0.5}$ models, indicating the importance of evaluating the goodness-of-fit for

each dataset individually. The two most prominent trends regard the growth conditions and the cell type.

First, SEI growth trends during storage ("calendar aging") generally have power-law exponents not too far from 0.5, although 0.5 only rarely falls within the 95% CIs of the fitted exponents. In contrast, SEI growth trends during cycling ("cycle aging") are almost always fit best by a generalized power law with an exponent less than 0.5. Bloom et al.[9] found the same result in their early studies of capacity fade: calendar aging scaled roughly with $t^{0.5}$, while cycle aging scaled with an exponent less than 0.5. This result is consistent with our theoretical description: while SEI growth is a complex phenomenon that is not necessarily strictly diffusion limited, SEI growth during storage, likely dominated by chemical SEI growth, is at least more consistent with standard film growth kinetics than SEI growth during cycling, which is likely dominated by electrochemical SEI growth.

Second, the two datasets where the $t^{0.5}$ model has the worst performance both consist of cycling carbon/lithium coin cells, with

Table I. Summary of literature review and fitting results. The fitted exponents are listed for the two-term and three-term power laws, respectively. All cells are aged at constant temperature (see text and references for additional details).

| Figure number in this work	References	Figure number in reference	Cell specifications	Aging conditions	SEI growth metric	Timescale (days)	Fitted exponents in power-law models (±95% CI)
4	Broussely et al.[7]	6	$LiNi_{0.81}Co_{0.09}O_2$/graphite [sic] cylindrical cells	Constant-voltage storage at 3.8 V	Capacity loss (%)	451	30 °C: 0.61 ± 0.02, 0.61 ± 0.02 60 °C: 0.53 ± 0.01, 0.48 ± 0.05
5	Wright et al.[10]	1	$LiNi_{0.8}Co_{0.2}O_2$/graphite cylindrical cells	Open-circuit storage (initially at 3.918 V)	Discharge resistance (R_{dis})	27	40 °C: N/A, 0.55 ± 0.04 50 °C: N/A, 0.55 ± 0.04 70 °C: N/A, 0.55 ± 0.02
6	Smith et al.[8]	7	Graphite/Li coin cells	Cycling (C/10 charge and discharge)	Total irreversible capacity (Q_{irr})	17	30 °C: 0.156 ± 0.002, 0.21 ± 0.01 40 °C: 0.175 ± 0.002, 0.267 ± 0.008 50 °C: 0.177 ± 0.006, 0.37 ± 0.04
7	Smith et al.[47]	8	$LiMn_2O_4$/graphite cylindrical cell	Cycling (C/14 charge and discharge)	Capacity loss (%)	48	40 °C: 0.68 ± 0.03, 0.48 ± 0.01
8	Fathi et al.[48]	2	$LiCoO_2$/graphite prismatic cells	Cycling (C/6 charge, C/150 discharge)	Capacity loss (%)	3,995	Group 3: 0.43 ± 0.01, 0.39 ± 0.03 Group 4: 0.413 ± 0.008, 0.35 ± 0.02
9	Attia et al.[26]	N/A	Carbon black/Li coin cells	Cycling (C/20 charge and discharge)	Total irreversible capacity (Q_{irr})	124	Cell 1: 0.205 ± 0.004, 0.08 ± 0.02 Cell 2: 0.195 ± 0.004, 0.053 ± 0.004 Cell 3: 0.194 ± 0.006, 0.011 ± 0.010
10	This work	N/A	Carbon black/Li coin cells	Open-circuit storage (initially at 0.01 V)	Self-delithiation capacity ($Q_{self-delith}$)	40	Cell 1: 0.339 ± 0.002, 0.226 ± 0.003 Cell 2: 0.401 ± 0.002, 0.311 ± 0.002 Cell 3: 0.4477 ± 0.0002, 0.4358 ± 0.0005
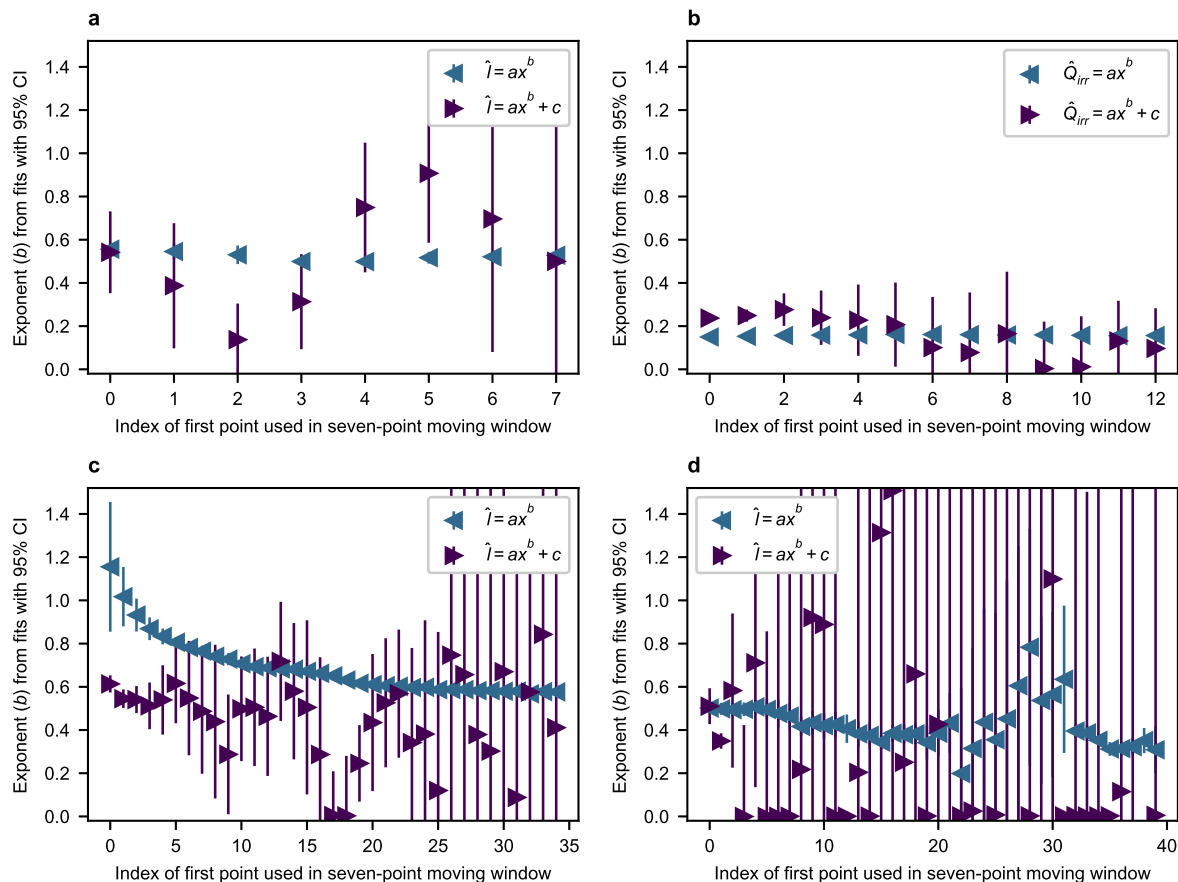
Figure 11. Power-law exponents from fits to subsets of four selected series: (a) Fig. 6 of Broussely et al.,[7] 60 °C series; (b) Fig. 7 of Smith et al.,[8] C/10 and 30 °C series; (c) Fig. 8 of Smith et al.,[47]; and (d) Fig. 2 of Fathi et al.,[48] Group 3. Seven points were used per fit, and the *x*-axis indicates the first index used in the seven-point moving window average. The power-law models used include $\hat{y} = at^b$ and $\hat{y} = at^b + c$. In all but one series, the exponents remain fairly constant using either model; in panel (c), the exponents in the two-term power law decrease smoothly from ∼1.2 to ∼0.6, although we note that this model performed poorly in Fig. 7. Additionally, the exponents of the $\hat{y} = at^b + c$ model generally have both much wider CIs and more variance as a function of the moving window due to the additional degree of freedom.

the SEI growth metric being the total irreversible capacity loss (the cumulative sum of the difference between charge and discharge capacities). These measurements are notable because they only capture SEI growth on the carbon electrode (and not on the lithium metal counter electrode). However, given that the $t^{0.5}$ model has little theoretical basis during cycling, we refrain from speculating on the origins of this observation. We note that in both cases, the estimated values of the exponents are much lower than 0.5 (∼0.2). In fact, most of the exponents from cycling datasets are less than 0.5, while most of the exponents from storage datasets are greater than 0.5.

We recognize that other effects may convolute these measurements of SEI growth, such as SEI growth on the positive electrode in full cells, active material loss, impedance growth, current inhomogeneity,[33] electrode interactions ("cross-talk"),[34–37] and overhang effects[38,39]; these effects may lead to the observed deviations from $t^{0.5}$ scaling. However, many of the selected datasets were designed specifically to measure SEI growth in isolation from other effects. In our own work on carbon black,[26] we detail why many of these effects are likely minor contributors at best. Furthermore, we emphasize that our claim in this section is simply that the existing empirical evidence for the $t^{0.5}$ growth of SEI is weak; future advances in SEI growth metrology may provide empirical evidence in favor of this model.

Transitions between different time regimes of SEI growth.—In our analysis, we use all data in each of the series to fit one model. However, the exponents in the power-law fits may vary locally in

time for either theoretical or empirical reasons. Theoretically, the SEI may exhibit transitions in its time scaling as the film grows—an idea that has been considered by the SEI modeling community.[11,14,15] These types of transitions are common in the oxidation literature.[19,20] In fact, even the simplest models of surface film growth (such as Deal-Grove) are initially reaction limited at low film thicknesses (yielding a linear time dependence for first-order reactions). Experimental measurements of first-cycle SEI growth demonstrate that the overpotential is exponential as a function of rate, indicating Butler-Volmer kinetics and an initial SEI limitation by surface reaction kinetics.[51] Empirically, power-law fits are often strongly influenced by the early time values and can easily overfit data with only 1–3 decades of temporal variation.[52]

In Fig. 11, we fit seven neighboring points at a time to both power-law expressions to examine the dependence of the fitted exponents as a function of cycle number in four series. This procedure can be thought of as a moving-window calculation with a window size of seven. In all but one series, the exponents remain fairly constant using either model; in panel (c), the exponents in the two-term power law decrease smoothly from ∼1.2 to ∼0.6, although we note that this model performed poorly in Fig. 7 and is likely an unreliable fit. This result suggests that the SEI does not experience major transitions in its time dependence beyond the first cycle or the formation procedure for the commercial cells, at least for these four data series.

We also find that the exponents are much more stable across cycle number ranges, and have much lower 95% CIs, using the
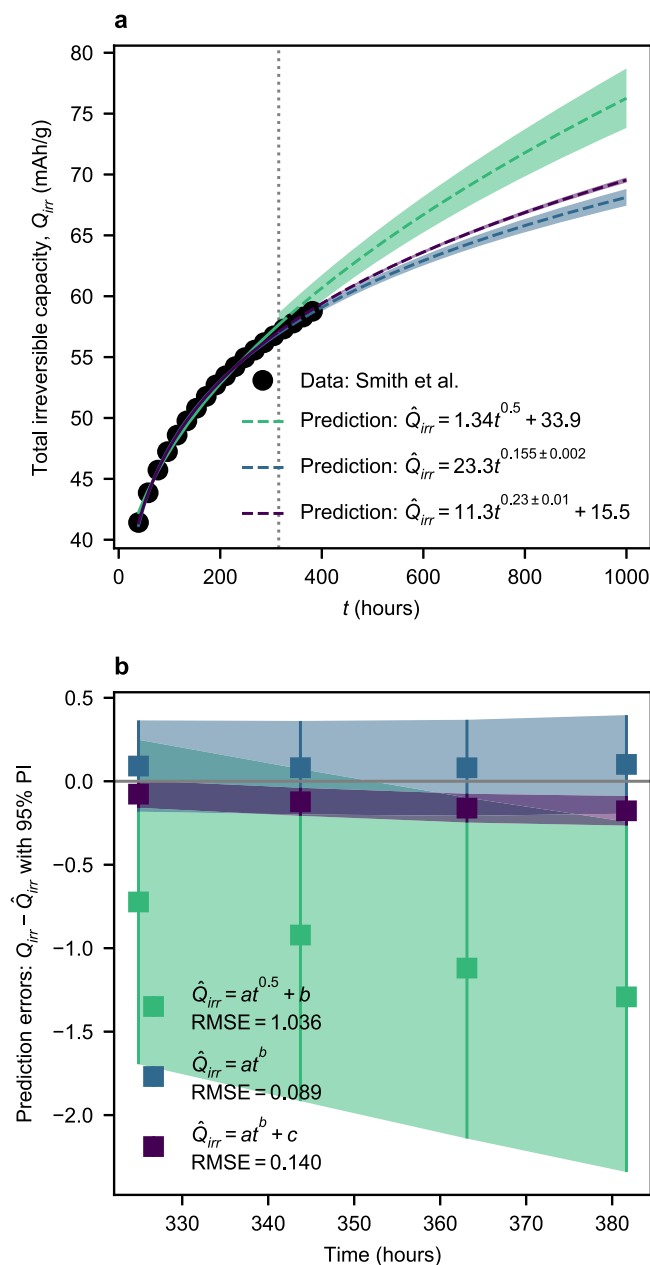
a

b

Figure 12. Comparison of predictions using $t^{0.5}$ and power-law fits to the data presented in Fig. 7 of Smith et al.[8] for graphite/lithium coin cells cycling at C/10 and 30 °C. (a) Irreversible capacity loss vs time and fits via three different models: $\hat{Q}_{irr} = at^{0.5} + b$, $\hat{Q}_{irr} = at^b$, and $\hat{Q}_{irr} = at^b + c$. The fits are performed using the first 80% of the data, i.e. the fifteen points to the left of the dotted line. The predicted trends of $\hat{Q}_{irr}$ at longer times from the three fits are also displayed, along with their 95% prediction intervals (possibly underestimated[54]). (b) Predictions of the last four data points using the three fits, along with their 95% prediction intervals. Only the two-term power-law model consistently produces predictions with prediction intervals that contain the true (measured) value; note that the three-term power-law model had a higher R^2_{adj} value when fitting all the data, illustrating how models that maximize *correlative* metrics may not maximize *predictive* metrics. The $t^{0.5}$ model exhibits the highest RMSE; in contrast, the power-law fits exhibit relatively small RMSEs. The error from the $t^{0.5}$ model rapidly grows with increasing time.

$\hat{Q}_{irr} = at^b$ model over the $\hat{Q}_{irr} = at^b + c$ model. The more complex model is quite sensitive to the specific data used given the low number of data points used for fitting (i.e. low number of degrees of freedom). In general, simpler models are recommended when few data points are available for fitting.

Predictions of future SEI growth.—A common use case for models of SEI growth is extrapolating into the future for lifetime prediction, which is essentially a time series forecasting problem.[53] For this use case, the choice of functional form is essential for accurate predictions. A simple approach for evaluating the predictive ability of candidate models is to fit to initial data, while holding out the final few points as a test set, and then to compare the root-mean-square error (RMSE) of the test set among various models.

Figure 12 illustrates this approach for the C/10, 30 °C series in Smith et al.[8] We selected this series for analysis to illustrate the dangers of using $t^{0.5}$ for prediction without comparing to multiple models. The model is trained on the initial 80% of the data (fifteen data points), while the final 20% of points are held out for testing (four data points). The RMSE of the test set is highest for the $t^{0.5}$ model. We also show the extrapolated trend lines at longer times in Fig. 4a, showing how $t^{0.5}$ overestimates the degradation as estimated by the power-law models. The additional predicted Q_{irr} from the $t^{0.5}$ model at 1000 hours is 66% larger than that of the two-term power-law model.

We also include the 95% prediction intervals in the figure; we note that these classical prediction intervals only incorporate uncertainty from the random error term, not the parameter estimates, and thus likely underestimate the error.[54] Only the two-term power-law model consistently produces predictions with prediction intervals that contain the true (measured) values in the test set. Interestingly, the three-term power-law model had a higher R^2_{adj} value when fitting all the data. This result illustrates how models that maximize *correlative* metrics may not maximize *predictive* metrics.

To empirically identify a suitable functional form for a dataset, we again propose the use of residual analysis. A fit without a systematic trend in the residuals will have low bias, which is particularly important for accurate predictions at long times. In Fig. S1, we investigate nine different functional forms fit to the same series (C/10, 30 °C) in Smith et al.[8] All functional forms considered exhibit a systematic trend in the residuals; however, the two $t^{0.5}$ models are among the lowest-performing candidate functional forms for this series. As previously discussed, SEI growth during cycling is not expected to follow $t^{0.5}$ scaling, so identifying a fit without systematic trends in the residuals may be challenging.

We end with a brief discussion of battery lifetime prediction. Broadly speaking, models of battery lifetime fall into one of three categories: first-principles, semi-empirical, and machine learning. In first-principles modeling, the only inputs are the physics and chemistry of battery degradation. In semi-empirical modeling (like that demonstrated here), the inputs are typically a combination of first-principles understanding and data from a single cell. Finally, in machine learning models, the inputs are data from many cells, perhaps with data transformations guided by battery domain knowledge. First-principles and semi-empirical models offer the ability to learn behavior over a broad range of operating conditions. However, their accuracy is predicated on our understanding of the relevant battery degradation modes. One implication of this work is that a previously established tenet of battery degradation—the $t^{0.5}$ scaling of SEI growth—is on less solid ground than previously believed. As such, machine learning methods are a compelling alternative in lieu of major advances in our understanding of battery degradation.

Conclusions

We reviewed the theoretical and experimental justification for $t^{0.5}$ models of SEI growth in lithium-ion batteries. Theoretically, the $t^{0.5}$ growth law only holds during steady-state growth—an assumption that may approximately hold during storage but rarely holds during typical cycling rates. The complexity of SEI growth also does not lend itself well to simple scaling relationships. Empirically, we found that $t^{0.5}$ scaling is not statistically justified in 16 of the 17 series investigated in this work. However, $t^{0.5}$ generally performs better for literature data measuring SEI growth during storage than for data measuring SEI growth during cycling. Finally, we found that

power-law exponents are relatively stable throughout different datasets, and we illustrated the pitfalls of using $t^{0.5}$ for capacity fade predictions without validating its applicability to the dataset of interest. We suggest that multiple models (certainly not restricted to power-law models) should be compared and evaluated via residual analysis—both for scientific claims of the time dependence of SEI growth and for extrapolation of capacity fade data in lifetime prediction applications.

Box[55] claimed that "all models are wrong, but some are useful." $t^{0.5}$ serves as a simple, straightforward model of the time dependence of SEI growth, but we hope this discussion leads to more useful models of SEI growth and more accurate predictions of battery lifetime.

Acknowledgments

ORCID

Peter M. Attia ⓘ https://orcid.org/0000-0003-4745-5726
William C. Chueh ⓘ https://orcid.org/0000-0002-7066-3470
Stephen J. Harris ⓘ https://orcid.org/0000-0002-5211-3934

References

1. E. Peled, *J. Electrochem. Soc.*, **126**, 2047 (1979).
2. M. Winter, *Z. Phys. Chem.*, **223**, 1395 (2009).
3. K. Xu, *Chem. Rev.*, **104**, 4303 (2004).
4. K. Xu, *Chem. Rev.*, **114**, 11503 (2014).
5. E. Peled and S. Menkin, *J. Electrochem. Soc.*, **164**, A1703 (2017).
6. Y. Li et al., *Science*, **358**, 506 (2017).
7. M. Broussely, S. Herreyre, P. Biensan, P. Kasztejna, K. Nechev, and ?R. J. Staniewicz, *J. Power Sources*, **97–98**, 13 (2001).
8. A. J. Smith, J. C. Burns, X. Zhao, D. Xiong, and J. R. Dahn, *J. Electrochem. Soc.*, **158**, A447 (2011).
9. I. Bloom et al., *J. Power Sources*, **101**, 238 (2001).
10. R. B. Wright et al., *J. Power Sources*, **110**, 445 (2002).
11. J. Christensen and J. Newman, *J. Electrochem. Soc.*, **151**, A1977 (2004).
12. M. Tang, S. Lu, and J. Newman, *J. Electrochem. Soc.*, **159**, A1775 (2012).
13. H. J. Ploehn, P. Ramadass, and R. E. White, *J. Electrochem. Soc.*, **151**, A456 (2004).
14. M. B. Pinson and M. Z. Bazant, *J. Electrochem. Soc.*, **160**, A243 (2013).
15. F. Single, B. Horstmann, and A. Latz, *J. Electrochem. Soc.*, **164**, E3132 (2017).
16. U. R. Evans, *Trans. Am. Electrochem. Soc.*, **46**, 247 (1924).
17. B. E. Deal and A. S. Grove, *J. Appl. Phys.*, **36**, 3770 (1965).
18. J. O. Bockris, A. K. N. Reddy, and M. E. Gamboa-Aldeco, *Modern Electrochemistry 2A: Fundamentals of Electrodics* (Springer, Boston, MA) 2nd ed. (2000).
19. N. Cabrera and N. F. Mott, *Rep. Prog. Phys.*, **12**, 163 (1949).
20. K. R. Lawless, *Rep. Prog. Phys.*, **37**, 231 (1974).
21. H. Z. Massoud, J. D. Plummer, and E. A. Irene, *J. Electrochem. Soc.*, **132**, 2685 (1985).
22. Y. Li and W. C. Chueh, *Annu. Rev. Mater. Res.*, **48**, 137 (2018).
23. S. E. Sloop, J. B. Kerr, and K. Kinoshita, *J. Power Sources*, **119–121**, 330 (2003).
24. B. Ravdel, K. M. Abraham, R. Gitzendanner, J. DiCarlo, B. Lucht, and C. Campion, *J. Power Sources*, **119–121**, 805 (2003).
25. C. L. Campion, W. Li, and B. L. Lucht, *J. Electrochem. Soc.*, **152**, A2327 (2005).
26. P. M. Attia, S. Das, S. J. Harris, M. Z. Bazant, and W. C. Chueh, *J. Electrochem. Soc.*, **166**, E97 (2019).
27. S. Das, P. M. Attia, W. C. Chueh, and M. Z. Bazant, *J. Electrochem. Soc.*, **166**, E107 (2019).
28. P. Keil, S. F. Schuster, J. Wilhelm, J. Travi, A. Hauser, R. C. Karl, and A. Jossen, *J. Electrochem. Soc.*, **163**, A1872 (2016).
29. F. Single, A. Latz, and B. Horstmann, *ChemSusChem*, **11**, 1950 (2018).
30. R. Metzler and J. Klafter, *Phys. Rep.*, **339**, 1 (2000).
31. S. Condamin, V. Tejedor, R. Voituriez, O. Bénichou, and J. Klafter, *PNAS*, **105**, 5675 (2008).
32. F. J. Anscombe, *The American Statistician*, **27**, 17 (1973).
33. S. J. Harris and P. Lu, *J. Phys. Chem. C*, **117**, 6481 (2013).
34. C. Delacourt, A. Kwong, X. Liu, R. Qiao, W. L. Yang, P. Lu, S. J. Harris, and V. Srinivasan, *J. Electrochem. Soc.*, **160**, A1099 (2013).
35. D. J. Xiong, L. D. Ellis, K. J. Nelson, T. Hynes, R. Petibon, and J. R. Dahn, *J. Electrochem. Soc.*, **163**, A3069 (2016).
36. B. Michalak, B. B. Berkes, H. Sommer, T. Brezesinski, and J. Janek, *J. Phys. Chem. C*, **121**, 211 (2017).
37. K. W. Knehr, T. Hodson, C. Bommier, G. Davies, A. Kim, and D. A. Steingart, *Joule*, **2**, 1146 (2018).
38. B. Gyenes, D. A. Stevens, V. L. Chevrier, and J. R. Dahn, *J. Electrochem. Soc.*, **162**, A278 (2015).
39. M. Lewerenz, J. Münnix, J. Schmalstieg, S. Käbitz, M. Knips, and D. U. Sauer, *J. Power Sources*, **345**, 254 (2017).
40. H. J. Motulsky and L. A. Ransnas, *The FASEB Journal*, **1**, 365 (1987).
41. M. L. Johnson, *Biophys. J.*, **44**, 101 (1983).
42. G. Kemmer and S. Keller, *Nat. Protoc.*, **5**, 267 (2010).
43. A. Rohatgi, (2019), WebPlotDigitizer.
44. B. U. Burda, E. A. O'Connor, E. M. Webber, N. Redmond, and L. A. Perdue, *Research Synthesis Methods*, **8**, 258 (2017).
45. D. Drevon, S. R. Fursa, and A. L. Malcolm, *Behav Modif*, **41**, 323 (2017).
46. P. M. Attia, *Time Dependence of SEI growth* (2019).
47. A. J. Smith, J. C. Burns, D. Xiong, and J. R. Dahn, *J. Electrochem. Soc.*, **158**, A1136 (2011).
48. R. Fathi, J. C. Burns, D. A. Stevens, H. Ye, C. Hu, G. Jain, E. Scott, C. Schmidt, and J. R. Dahn, *J. Electrochem. Soc.*, **161**, A1572 (2014).
49. W. Huang et al., *Nano Lett.*, **19**, 5140 (2019).
50. M. D. Levi, C. Wang, and D. Aurbach, *J. Electrochem. Soc.*, **151**, A781 (2004).
51. D. Goers, M. E. Spahr, A. Leone, W. Märkle, and P. Novák, *Electrochim. Acta*, **56**, 3799 (2011).
52. A. Clauset, C. R. Shalizi, and M. E. J. Newman, *SIAM Rev.*, **51**, 661 (2009).
53. R. J. Hyndman and G. Athanasopoulos, *Forecasting principles and practice* (O Texts, online open-access textbooks, Melbourne) (2018).
54. R. J. Hyndman, A. B. Koehler, R. D. Snyder, and S. Grose, *Int. J. Forecast.*, **18**, 439 (2002).
55. G. E. P. Box, *J. Am. Stat. Assoc.*, **71**, 791 (1976).